The EMBO Journal Vol. 20 No. 24 pp. 7008–7021, 2001

Polarized trafficking and surface expression of the AQP4 water channel are coordinated by serial and regulated interactions with different clathrin–adaptor complexes

Ricardo Madrid, Sophie Le Maout, Marie-Bénédicte Barrault, Katy Janvier[1], Serge Benichou[1] and Jean Mérot[2,3]

Service de Biologie Cellulaire, Département de Biologie Cellulaire et Moléculaire, CEA/Saclay, F-91191 Gif-sur-Yvette, Cedex, [1]Institut Cochin de Génétique Moléculaire, INSERM U529, F-75014 Paris and [2]INSERM U533, Faculté de Médecine, F-44093 Nantes, France

[3]Corresponding author
e-mail: jean.merot@nantes.inserm.fr

R.Madrid and S.Le Maout contributed equally to this work

Aquaporin 4 (AQP4) is the predominant water channel in the brain. It is targeted to specific membrane domains of astrocytes and plays a crucial role in cerebral water balance in response to brain edema formation. AQP4 is also specifically expressed in the basolateral membranes of epithelial cells. However, the molecular mechanisms involved in its polarized targeting and membrane trafficking remain largely unknown. Here, we show that two independent C-terminal signals determine AQP4 basolateral membrane targeting in epithelial MDCK cells. One signal involves a tyrosine-based motif; the other is encoded by a di-leucine-like motif. We found that the tyrosine-based basolateral sorting signal also determines AQP4 clathrin-dependent endocytosis through direct interaction with the μ subunit of AP2 adaptor complex. Once endocytosed, a regulated switch in μ subunit interaction changes AP2 adaptor association to AP3. We found that the stress-induced kinase casein kinase (CK)II phosphorylates the Ser276 immediately preceding the tyrosine motif, increasing AQP4–μ3A interaction and enhancing AQP4–lysosomal targeting and degradation. AQP4 phosphorylation by CKII may thus provide a mechanism that regulates AQP4 cell surface expression.

Keywords: adaptor protein complex/AQP4/phosphorylation/protein sorting/regulated membrane trafficking

Introduction

Aquaporin water channels are essential for mediating rapid osmotic water transport across cell membranes. The product of at least one of the 10 distinct mammalian aquaporin genes has been identified in nearly all tissues, reflecting the fundamental nature of water transport processes. The ubiquitous character of aquaporins is associated with remarkably conserved structural features. Structural and functional analyses have revealed that aquaporins are homomultimeric complexes containing four identical subunits. All the aquaporin subunits identified to date have N- and C-termini facing the cytosol, and contain six transmembrane domains that are connected by five loops (Deen and van Os, 1998; Engel *et al*., 2000). Multiple aquaporins are often expressed in a single cell on different subcellular membrane domains where they are subjected to distinct regulatory cues. Although the phenomenon underlies a plethora of physiologically relevant water transport processes, little is known about the molecular mechanisms that govern the membrane targeting and expression of aquaporin channels.

Consider, for example, the epithelial renal collecting duct principal cell and the cellular basis for the regulation of water balance. These cells express at least three different types of aquaporins in a polarized fashion. The vasopressin-regulated aquaporin 2 (AQP2) is specifically targeted to the apical cell domain. The hormone induces insertion of a vesicular pool of AQP2 channels in the apical membranes to allow efficient transcellular osmotic water re-absorption to occur in accord with physiological demands (Brown *et al*., 1988). The two other water channels, AQP3 and AQP4, are expressed on the basolateral membrane (Deen and van Os, 1998; Brown and Breton, 2000). Consistent with a more widespread targeting mechanism, AQP4 is also specifically targeted to the basolateral membranes of a variety of different epithelial cells, including the renal proximal tubule, the parietal cell in the stomach and the trachea (Frigeri *et al*., 1995; Fujita *et al*., 1999; van Hoek *et al*., 2000).

The differential targeting and regulation of aquaporins on distinct membrane domains is not an exclusive property of epithelial cells. For instance, AQP4 membrane expression is also polarized in brain glial cells. Immunolocalization studies revealed that, in astrocytes, AQP4 is targeted to membrane endfoot processes that juxtapose blood vessels, where it forms dense orthogonal arranged particle arrays (OAPs) (Nagelhus *et al*., 1998; Rash *et al*., 1998). In the eye, Muller cells target AQP4 to restricted membrane domains together with the potassium channel (Kir 4.1) (Nagelhus *et al*., 1999), where it may facilitate water fluxes accompanying potassium siphoning. In the brain, AQP4 is involved in many physiological processes, including K^+ buffering, body fluid homeostasis, central osmoreception and cerebrospinal fluid formation (Jung *et al*., 1994; Venero *et al*., 2001). Recent studies have also unveiled its crucial role in response to brain edema formation after osmotic, traumatic and ischemic insults (Manley *et al*., 2000; Vajda *et al*., 2000; Ke *et al*., 2001).

Analysis of protein targeting in polarized cells has been most extensively studied in epithelial cells. Proteins destined for the basolateral membrane contain short peptidic signals in their cytoplasmic domains that specify the segregation and targeting of vesicles to the appropriate membrane domain. To date, different determinants, including single aromatic amino acid residues, di-hydrophobic or tyrosine-based motifs, have been identified as

 Published by Oxford University Press

targeting signals in several basolateral proteins (Heilker *et al*., 1999; Yeaman *et al*., 1999). Likewise, it is well established that tyrosine-based (YxxΦ) and di-leucine-based signals are also involved in different trafficking steps of membrane proteins as they interact with one or more of the heterotetrameric adaptor complexes AP1, AP2 and AP3. AP1 is responsible for the traffic of proteins between the *trans*-Golgi network (TGN) and endosomal compartments, AP2 mediates endocytosis from the plasma membrane, and AP3 is involved in protein targeting to lysosomes. Their respective medium subunits μ1, μ2 and μ3 interact directly with the tyrosine motifs, while di-leucine-based signals have been shown to interact with μ1 and μ2, as well as an additional adaptor complex subunit, β1 (Rapoport *et al*., 1998). Whether these mechanisms are involved in the polarized membrane targeting and trafficking of aquaporins remains unknown.

In the present study, we have examined the polarized trafficking and surface expression of AQP4 in MDCK cells, a model kidney epithelial cell line. We have identified a unique 30-amino-acid sorting cassette within the cytoplasmic C-terminus of AQP4. This domain contains several distinct sorting signals that co-ordinate basolateral delivery and regulate surface expression by endocytosis and lysosomal degradation through serial interactions with different clathrin–adaptor protein complexes.

Results

AQP4 is targeted to the basolateral membranes of MDCK cells

Before AQP4 sorting determinants were elucidated, biochemical and immunolocalization experiments were performed on MDCK cells stably transfected with wild-type and VSV-tagged AQP4 cDNAs to ascertain that: (i) the VSV epitope tag introduced at the N-terminus of the protein did not impede AQP4 processing, assembly or routing; and (ii) the MDCK cells constitute an appropriate cellular model to analyze AQP4 polarized trafficking. Western blot experiments (Figure 1A) using anti-AQP4 antibody (Valenti *et al*., 1996) specifically identified a major band with the expected apparent molecular weight of AQP4 (~34 kDa) in wild-type (WT) (lane 2) and VSV-AQP4 (lane 3) transfected MDCK cells, but not in control untransfected cells (lane 1). Insensitivity to glycopeptidase F treatment (lane 4) indicated that AQP4 was not glycosylated in MDCK cells. Additional ~60 and ~97 kDa bands, which most probably represent SDS-insoluble AQP4 oligomers (Neely *et al*., 1999), were also detected. Differential velocity sedimentation centrifugation on a 5–20% sucrose gradient and cross-linking experiments confirmed that AQP4 assembles into homomultimers in MDCK cells (our unpublished data).

AQP4 distribution in the apical and basolateral membranes of polarized MDCK cells was evaluated by specific membrane biotinylation experiments and confocal microscopy. As shown in Figure 1B, 95% of WT-AQP4 and 98% of VSV-AQP4 were detected in the basolateral fraction of biotinylated plasma membrane proteins. Confocal microscopy analysis corroborated this observation (Figure 1C). Both proteins were restricted to the basolateral plasma membrane domain of the cells, as

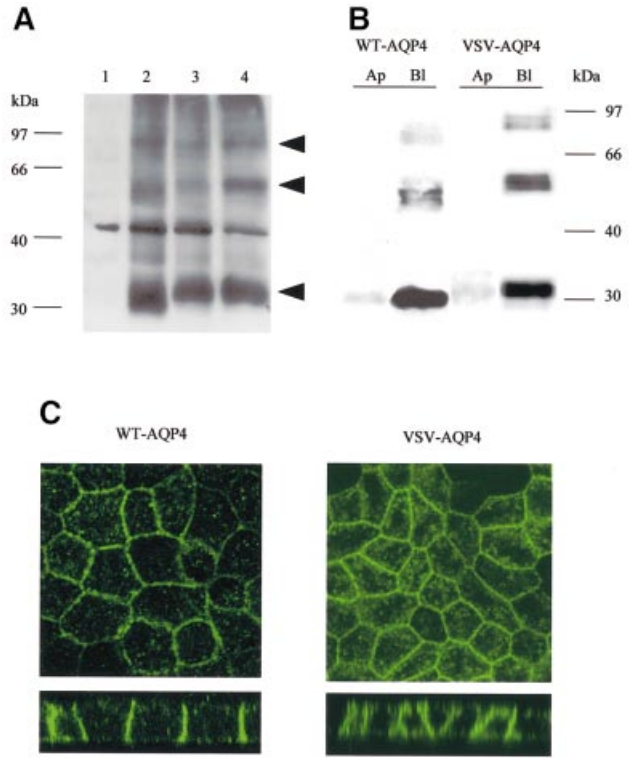

Fig. 1. Western blot and immunolocalization analysis of AQP4 in MDCK cells. (**A**) Western blot probed with anti-AQP4 antibody. Lane 1: control MDCK cells, lane 2: wild-type AQP4, lane 3: VSV-AQP4 transfected MDCK cells. Glycopeptidase F treatment did not affect VSV-AQP4 MW indicating the protein was not glycosylated (lane 4). Arrowheads indicate 34, 60, 97 kDa bands specifically detected. (**B**) Steady-state repartition of AQP4 in apical and basolateral membranes. Western blot of plasma membrane fraction of WT and VSV-AQP4 cells biotinylated from the basolateral (Bl) and the apical (Ap) side growing on a permeable support and probed with anti-AQP4 antibody. (**C**) Confocal images of WT and VSV-AQP4 protein stably transfected in MDCK cells and detected using anti-AQP4 and VSV antibodies, respectively. The upper and lower images show focal planes parallel and perpendicular to the epithelium, respectively.

described *in vivo* in gastric and kidney epithelial cells. Interestingly, accumulation of AQP4 in intracellular structures was also observed (see Figure 1C and below).

Collectively, these results show that (i) the VSV tag does not affect the post-translational processing and assembly of AQP4 protein, and (ii) AQP4 is targeted to the basolateral membranes of the cells. Thus, MDCK cells represent an appropriate *in vitro* cellular model system to analyze the molecular determinants of AQP4 basolateral targeting.

AQP4 C-terminus contains two independent basolateral sorting signals

Protein sequence alignment of the differentially targeted aquaporin channels revealed important divergences within their cytoplasmic C-terminal domains (Deen and van Os, 1998). Interestingly, the AQP4 C-terminus harbors several conspicuous structural features that could constitute potential basolateral membrane sorting determinants. We thus focused our attention on the AQP4 cytoplasmic tail and analyzed the effects of sequential C-terminal deletions on AQP4 basolateral targeting (Table I).

Table I. C-terminal amino acid sequences of wild-type and mutated AQP4

Construct	AQP4 C-terminal sequence.	Figure
	261 271 281 291 301 311 321	
VSV-AQP4	RLKEAFSKAAQQTKGSYMEVEDNRSQVETEDLILKPGVVHVIDIDRGDEKKGKDSSGEVLSSV	Fig 1C
321 Stop	RLKEAFSKAAQQTKGSYMEVEDNRSQVETEDLILKPGVVHVIDIDRGDEKKGKDSSGEVL	Fig 2A
303 Stop	RLKEAFSKAAQQTKGSYMEVEDNRSQVETEDLILKPGVVHVI	Fig 2A
282 Stop	RLKEAFSKAAQQTKGSYMEVE	Fig 2A
272 Stop	RLKEAFSKAAQ	Fig 2A
Δ272-302	RLKEAFSKAAQ----------DIDRGDEKKGKDSSGEVLSSV	Fig 2B
Δ272-281	RLKEAFSKAAQ----------DNRSQVETEDLILKPGVVHVIDIDRGDEKKGKDSSGEVLSSV	Fig 2B
Δ282-302	RLKEAFSKAAQQTKGSYMEVE----------DIDRGDEKKGKDSSGEVLSSV	Fig 2B
Y277A,Δ282-302	RLKEAFSKAAQQTKGS**A**MEVE----------DIDRGDEKKGKDSSGEVLSSV	Fig 3A
V280S,Δ282-302	RLKEAFSKAAQQTKGSYME**S**E----------DIDRGDEKKGKDSSGEVLSSV	Fig 3A
GY-AA,Δ282-302	RLKEAFSKAAQQTK**AS**AMEVE----------DIDRGDEKKGKDSSGEVLSSV	Fig 3B
SY-AA,Δ282-302	RLKEAFSKAAQQTKG**AA**MEVE----------DIDRGDEKKGKDSSGEVLSSV	Fig 3B
GSY-AAA,Δ282-302	RLKEAFSKAAQQTK**AAA**MEVE----------DIDRGDEKKGKDSSGEVLSSV	Fig 3B
Δ272-286	RLKEAFSKAAQ----------VETEDLILKPGVVHVIDIDRGDEKKGKDSSGEVLSSV	Fig 4A
Δ272-290	RLKEAFSKAAQ----------DLILKPGVVHVIDIDRGDEKKGKDSSGEVLSSV	Fig 4A
Δ272-294	RLKEAFSKAAQ----------KPGVVHVIDIDRGDEKKGKDSSGEVLSSV	Fig 4A
GSY-AAA,ETDE-AAAA	RLKEAFSKAAQQTK**AAA**MEVEDNRSQV**AAAA**LILKPGVVHVIDIDRGDEKKGKDSSGEVLSSV	Fig 4B
GSY-AAA,LIL-AAA	RLKEAFSKAAQQTK**AAA**MEVEDNRSQVETED**AAA**KPGVVHVIDIDRGDEKKGKDSSGEVLSSV	Fig 4B
GSY-AAA,ETDEDLIL-7xA	RLKEAFSKAAQQTK**AAA**MEVEDNRSQV**AAAAAAA**KPGVVHVIDIDRGDEKKGKDSSGEVLSSV	Fig 4B
Y277A	RLKEAFSKAAQQTKGS**A**MEVEDNRSQVETEDLILKPGVVHVIDIDRGDEKKGKDSSGEVLSSV	Fig 6A
S276D	RLKEAFSKAAQQTKG**D**YMEVEDNRSQVETEDLILKPGVVHVIDIDRGDEKKGKDSSGEVLSSV	Fig 8E
S276A	RLKEAFSKAAQQTKG**A**YMEVEDNRSQVETEDLILKPGVVHVIDIDRGDEKKGKDSSGEVLSSV	
SSS-AAA	RLKEAFSKAAQQTKG**A**YMEVEDNR**A**QVETEDLILKPGVVHVIDIDRGDEKKGKD**A**SGEVLSSV	
V280S	RLKEAFSKAAQQTKGSYME**S**EDNRSQVETEDLILKPGVVHVIDIDRGDEKKGKDSSGEVLSSV	

C-terminal amino acid sequences of wild-type and AQP4 mutants from arginine 261 (R261) to terminal valine (V323). Amino acid substitutions and deletions are shown in bold letters and dashes, respectively. Figures showing confocal microscopy images of the different mutants are indicated in the right-hand column.

Deletion of the last three amino acids, which comprise a potential PDZ binding motif (Sheng and Kim, 2000), or the terminal 21 or 42 amino acids which contain leucine-based and acidic motifs, did not alter AQP4 basolateral expression (Table I, AQP4-321 Stop, 303 Stop and 282 Stop, respectively) (Figure 2A). However, a larger deletion (AQP4-272 Stop), including a potential tyrosine-based motif, caused a profound modification of AQP4 localization. As illustrated in Figure 2A, the basolateral plasma membrane expression was no longer detectable and the protein was concentrated in intracellular perinuclear compartments. On the other hand, internal deletion of the 31 amino acids in the central part of the AQP4 tail resulted in the routing of >90% of the aquaporin to the apical membranes (Table I; AQP4 Δ272–302, Figure 2B). This result identifies the 31-amino-acid sequence between Q272 and I302 as the basolateral targeting determinant of AQP4. When either the initial or the terminal part of this sorting domain was deleted (AQP4 Δ272–281 and AQP4 Δ282–302, respectively), the mutant protein was still expressed in the basolateral membranes of the cells (Figure 2B). It must be noted that the deletion of the initial sequence (Δ272–281) also resulted in intense basolateral staining and a reduced intracellular labeling. Together, this suggested that the AQP4 basolateral targeting cassette contains two independent basolateral sorting signals encoded in the amino acid regions Q272-//-E281 and D282-//-I302.

The proximal basolateral sorting signal involves a tyrosine-based sorting motif

Examination of the proximal sorting signal sequence (272-QTKGSYMEVE-281) revealed a putative tyrosine-based motif (YxxΦ) similar to the basolateral sorting signal of several other membrane proteins. To address its role in AQP4 basolateral targeting, Tyr277 (Y277) and Val280

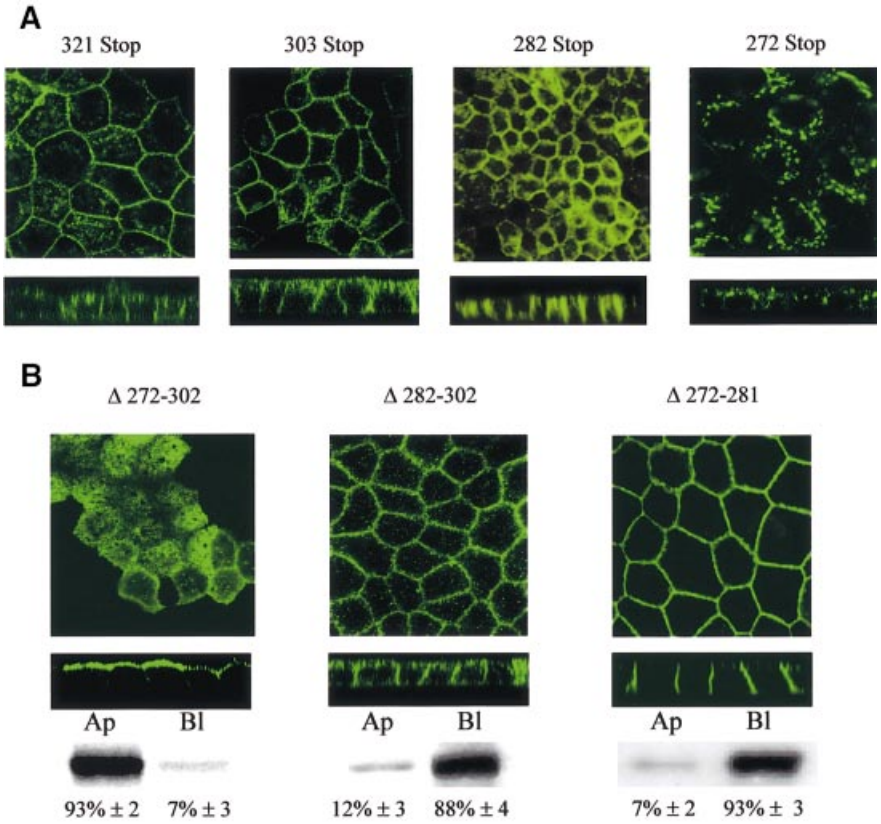

Fig. 2. Two independent motifs determine AQP4 basolateral targeting. (**A**) Confocal microscopy images of VSV-AQP4 mutants missing the 3 (321 Stop), 21 (303 Stop), 42 (282 Stop) and 52 (272 Stop) C-terminal amino acids, respectively. (**B**) Confocal microscopy images of AQP4-Δ272–302, Δ272–281 and Δ282–302 mutants bearing internal deletion of 31, 10 and 21 amino acid residues, respectively. An example of quantification of apical versus basolateral expression of the mutants by specific membrane biotinylation and western blotting (see Materials and methods) is shown together with the mean ± SD of at least three experiments.

(V280) were mutated to alanine and serine, respectively. These substitutions were introduced in the AQP4 Δ282–302 construct in which the second basolateral sorting signal was deleted. As illustrated in Figure 3A, Δ282–302,Y277A and AQP4 Δ282–302,V280S were preferentially targeted to the apical membranes (81 and 72%, respectively). This result identifies the tyrosine motif as a critical determinant of the AQP4 basolateral sorting signal. It suggests, however, that additional amino acids surrounding the tyrosine motif are also involved. The role of glycine and serine residues (G275 and S276) preceding Y277 was investigated by alanine substitution. As illustrated in Figure 3B, G,Y-A,A and GSY-AAA but not SY-AA substitutions resulted in 97, 92 and 78% apical targeting, respectively. This indicates that Ser276 does not play a key role in AQP4 basolateral targeting. Conversely, the tyrosine motif and the preceding glycine residue are critical components of the proximal basolateral signal of AQP4.

The distal basolateral sorting signal involves a di-leucine-based motif preceded by an acidic cluster

The results presented above (Figure 2) show that the second basolateral sorting determinant is positioned between Asp282 (D282) and the Ile302 (I302) residues (Table I). To define the sorting motif more precisely, sequential deletions in the amino acid stretch 282-DNRSQVETEDLILKPGVVHVI-302 were made in an AQP4 Δ272–281 mutant, which lacks the tyrosine-based sorting signal (Table I). The deletion of the five initial amino acid residues (DNRSQ) did not affect AQP4 basolateral targeting (Figure 4A, AQP4 Δ272–286). In contrast, deletion of four additional residues (VETE) resulted in 75% routing to the apical membranes (Figure 4A, AQP4 Δ272–290). Total apical targeting (>95%) was observed when the triplet LIL was also deleted (AQP4 Δ272–294). To ensure that the results reported above were not biased by the shortening of the AQP4 C-terminus, the effects of alanine substitutions were tested in full-length AQP4 in which the proximal sorting motif was disrupted by GSY-AAA mutation. Alanine substitution of either the acidic cluster (ETED) or the leucine-based motif (LIL) resulted in a non-polarized distribution in both apical and basolateral membranes (Figure 4B, AQP4-GSY-AAA, ETED-AAAA and LIL-AAA, respectively). However, the acidic cluster substitution determined a more important re-routing to the apical membranes than the LIL motif (81 and 60%, respectively). On the other hand, simultaneous substitution of both produced a definite apical targeting of AQP4 (Figure 4B, AQP4-GSY-AAA, ETEDLIL-7×A). Together, these data establish that the distal sorting determinant is encoded by the amino acid sequence 288-ETEDLIL-294.

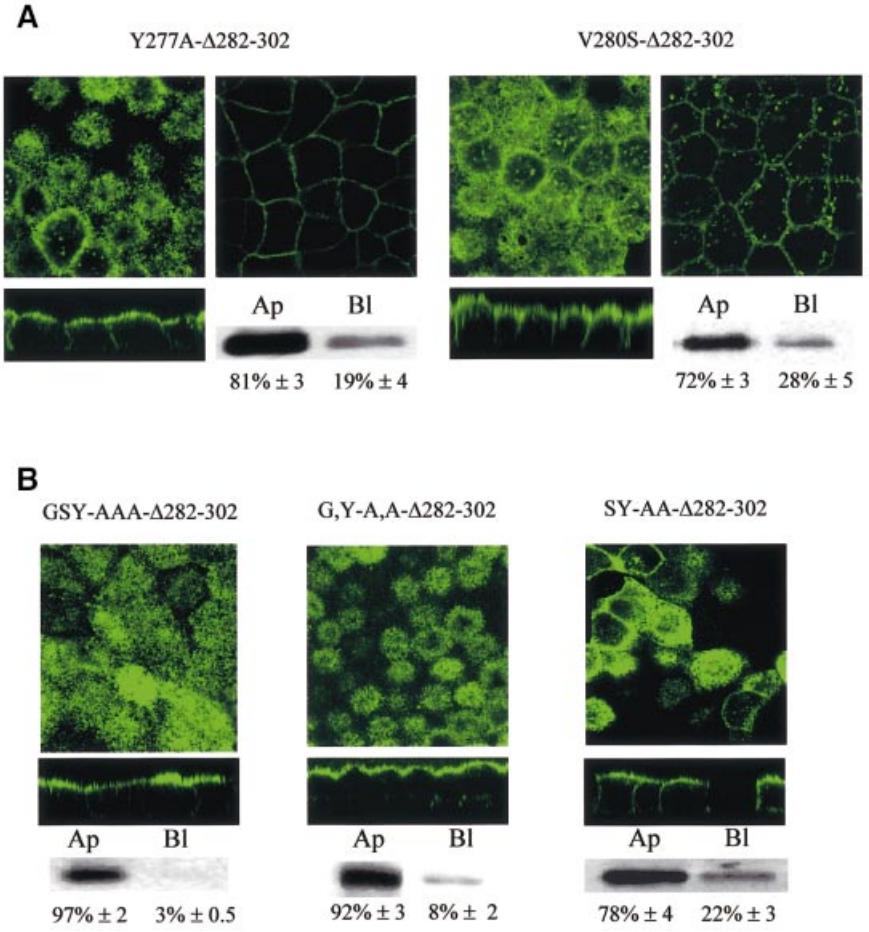

Fig. 3. The proximal basolateral sorting signal juxtaposes a tyrosine motif. Confocal microscopy images of VSV-AQP4 mutants bearing Y277A and V280S point mutations in the tyrosine motif (GSYMEV) (**A**) or GSY-AAA and G,Y-A.A and SY-A.A substitutions (**B**). All these mutations were introduced in the backbone construct AQP4-Δ282–302 in which the second basolateral sorting signal was deleted. Two different focal planes taken at the level of the apical and basolateral membranes of the same cells are shown in (A). Apical versus basolateral repartition was quantified by specific membrane biotinylation and western blotting (see legend to Figure 2).

The tyrosine motif determines AQP4 clathrin-mediated endocytosis

Inspection of the subcellular localization of AQP4 mutants missing the YxxΦ motif revealed that, independently of the target membrane, intense staining of the plasma membranes was observed with little intracellular staining compared with wild-type AQP4 (see Figures 1C, 2B, 3 and 4). This suggests that the tyrosine motif is not involved in AQP4 plasma membrane delivery but rather along its endocytic pathway.

A biotinylation assay was used to analyze AQP4 endocytosis. Plasma membrane AQP4 was labeled with a cleavable biotin analog (NHS-SS-biotin) at 4°C and internalized for 15 min at 37°C. The extracellular biotin was removed by cleaving the disulfide linkage with glutathione, and the amount of labeled AQP4 resistant to glutathione reduction was taken as a measure of its internalization (Figure 5A). As reported in Figure 5B, 25% of plasma membrane AQP4 was internalized in 15 min. In addition, we showed that hypertonic shock (sucrose 0.45 M), a treatment known to perturb clathrin-mediated endocytosis (Hansen *et al.*, 1993), significantly reduced AQP4 internalization (Figure 5B). The critical role of the tyrosine motif was demonstrated by the ~80% decrease in endocytosis rates measured for both AQP4-Y277A and AQP4-V280S mutants (Figure 5B).

To determine whether the μ subunit of AP2 clathrin–adaptor complex was involved in AQP4 internalization through direct recognition of the YMEV tyrosine motif, AQP4-μ2 interaction was tested using glutathione *S*-transferase (GST)–AQP4-Cter fusion protein and *in vitro* translated ^{35}S-labeled μ2 subunit and a yeast two-hybrid interaction assay. As illustrated in Figure 5C, μ2 protein was specifically retained by GST–AQP4, but not by GST alone. The interaction critically depended on the tyrosine motif as neither GST–AQP4-Y277A nor GST–AQP4-V280S retained μ2. These results were confirmed in a yeast two-hybrid interaction assay. Indeed, the AQP4 C-terminus interacted with the μ2 subunit, whereas Y277A and V280S mutants did not (Figure 5D).

Collectively, these data strongly suggest that AQP4 is endocytosed via clathrin-mediated mechanisms through direct protein–protein interactions between the tyrosine motif YMEV and the μ subunit of the AP-2 complex.

AQP4 is targeted to lysosomes and interacts with the μ3A subunit of the AP3 complex

Once endocytosed, AQP4 may either recycle back to the plasma membrane or enter the late endocytic pathway

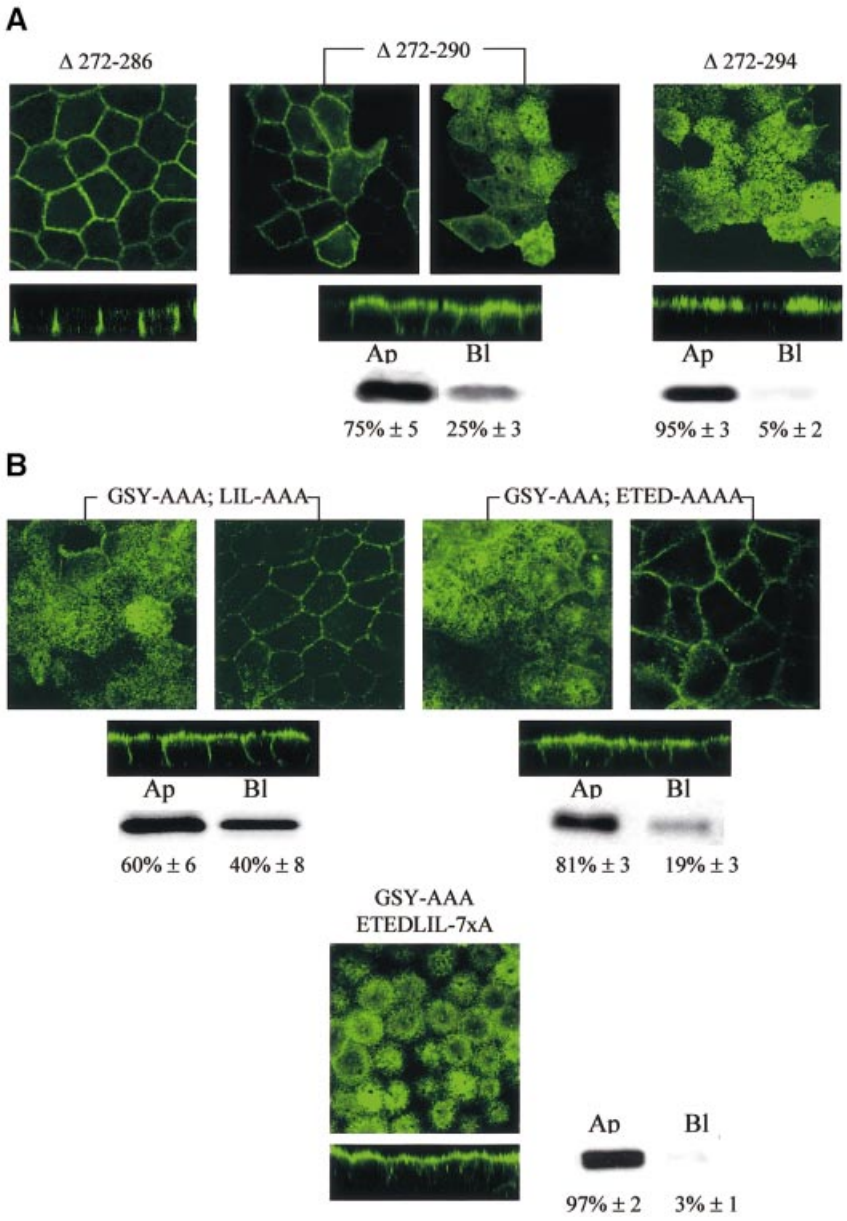

Fig. 4. Di-leucine-like and acidic cluster constitute the second basolateral sorting signal. (**A**) Confocal microscopy images of VSV-AQP4 mutants bearing increasing deletions of DNRSQ, VETE and LIL in the DNRSQVETEDLILKPGVVHVI sequence (Δ272–286, Δ272–290 and Δ272–294, respectively). (**B**) Simultaneous (ETEDLIL-7×A) but not serial alanine substitution of the acidic cluster (ETED-AAA) and the leucine like motif (LIL-AAA) was necessary to target AQP4 to the apical membranes. Two different focal planes taken at the level of the apical and basolateral membranes of the same cells are shown in (A) and (B). In mutants shown in (A) and (B), the tyrosine-based basolateral sorting motif was removed by deletion (Δ272–281) and GSY-AAA substitution, respectively. Apical versus basolateral repartition was quantified by biotinylation and western blotting (see legend to Figure 2).

down to the lysosome to be degraded. Consistent with the latter hypothesis, we found that intracellular wild-type AQP4, but not AQP4-Y277A, largely co-localized with the late endosome/lysosomal marker LampI (Figure 6A). The impaired endocytosis and lysosomal targeting of Y277A mutant were correlated with a reduced degradation rate, as observed in pulse–chase experiments (Figure 6B). Thus, it appears that a significant fraction of internalized AQP4 is not recycled to the plasma membrane, but is, instead, targeted to and degraded into lysosomes.

Lysosomal targeting of several internalized plasma membrane proteins is specified by direct interaction with the μ subunit of the AP3 complex (Le Borgne *et al*., 1998; Odorizzi *et al*., 1998). The results shown in Figure 6B and C indicate that wild-type AQP4 is able to interact directly with the μ subunit of the AP3 complex. *In vitro* translated μ3A is retained by GST–AQP4-Cter fusion protein and we found that the interaction critically depended on the tyrosine motif since neither GST–AQP4-Y277A nor GST–AQP4-V280S mutants retained μ3A (Figure 6C). These results were confirmed and quantified using the β-galactosidase reporter activity in a yeast two-hybrid interaction assay. The AQP4 C-terminus fused to the LEXA binding domain interacted with the μ3A subunit

fused to the Gal4 activation domain, whereas Y277A and V280S mutants did not (Figure 6D). These experiments reveal that AQP4 interacts, via its cytoplasmic tyrosine motif, with the μ3A subunit of the AP3 complex.

Casein kinase II phosphorylates AQP4 and modulates AQP4–μ3A interaction

Previous studies have revealed that the nature of the residues surrounding tyrosine motifs is a major determinant of their interaction with μ subunits of AP complexes (Ohno *et al*., 1996). Interestingly, the serine in position Y-1 (Ser276) lies in a casein kinase II (CKII) consensus site. If this residue is indeed phosphorylated and thus negatively charged, the tyrosine motif would perfectly match the consensus sequence favored by the μ3A subunit (Figure 7A) (Ohno *et al*., 1998), suggesting that AQP4 lysosomal targeting may be regulated by phosphorylation. To test this hypothesis, we analyzed (i) AQP4 phosphorylation by CKII, and (ii) the relative strength of interaction between μ3A and an AQP4 mutant in which Ser276 was replaced by an aspartic acid (AQP4-S276D) to mimic serine phosphorylation using the yeast two-hybrid assay.

The results presented in Figure 7A show that ^{32}P-labeled AQP4 was specifically immunoprecipitated from VSV-AQP4-MDCK cells incubated for 2 h in the presence of ^{32}P-labeled orthophosphate. The involvement of CKII in AQP4 phosphorylation was established by two observations. First, AQP4 phosphorylation was heavily reduced when the three potential CKII consensus sites present in its C-terminal domain were suppressed by alanine substitutions (Table I, AQP4-SSS-AAA) (Figure 7A). Secondly, AQP4 immunopurified from WT or VSV-AQP4-MDCK cells was phosphorylated *in vitro* by recombinant human CKII in the presence of [^{32}P]ATP (Figure 7B, left panel). To determine whether Ser276 is an actual CKII substrate, we used GST–AQP4-Cter proteins in which only one out of the three C-terminal CKII consensus sites was sequentially conserved (Ser276, Ser285 and Ser315, respectively). Figure 7B (right panel) shows that the three serine residues, including Ser276, were indeed efficiently phosphorylated by CKII.

Next, we wanted to know whether the phosphorylation status of Ser276 could modulate AQP4 interaction with the μ3A subunit. Figure 7C shows that S276A substitution did not modify their apparent strength of interaction measured using the yeast two-hybrid assay. Interestingly, the S276D substitution used to mimic phosphorylation increased the strength of the interaction >5-fold. Altogether, these results show that Ser276 is a substrate for CKII and that Ser276 phosphorylation increases AQP4–μ3A interaction.

Ser276 phosphorylation modulates AQP4 lysosomal targeting

The effects of Ser276 phosphorylation on AQP4 trafficking and fate were then analyzed. Pulse–chase experiments coupled to cell surface biotinylation revealed that AQP4 and S276D were both delivered to the cell plasma membrane efficiently (Figure 8A). Ser276 phosphorylation status did not affect AQP4 interaction with the μ2 subunit and AQP4 endocytosis either. As shown in Figure 8B and C, *in vitro* translated μ2 protein was retained by both GST–S276A and S276D mutants (Figure 8B), and endocytosis rates of the two mutants measured in MDCK cells were not different from that of wild-type AQP4 (Figure 8C). In contrast, as expected from the strengthening of the μ3A–AQP4 interaction described above, AQP4-S276D exhibited an increased degradation rate with respect to both wild type and AQP4-S276A mutant (Figure 8D). This higher degradation rate of AQP4-S276D was associated with an increased co-localization with the LampI marker and decreased plasma membrane labeling (Figure 8E).

Together, these data show that Ser276 phosphorylation does not affect AQP4 delivery to the plasma membrane nor internalization from the cell surface, but does modulate its targeting to the late degradation compartments of the endocytic pathway. AQP4 phosphorylation by CKII may thus provide a mechanism that regulates AQP4 cell surface expression.

Discussion

In the present study, we identified a 31-amino-acid sorting cassette in the cytoplasmic C-terminal domain of the water channel AQP4. This cassette carries several instructions specifying basolateral membrane targeting and intracellular trafficking of the protein. A unique tyrosine sorting signal is designed to coordinate a stepwise series of interactions with different clathrin–adaptor complexes for sequential endocytosis and routing to lysosomes. Furthermore, we found that phosphorylation by CKII can modulate the trafficking and the degradation of AQP4 and thus participate to a sequential program of regulated surface expression of the water channel. Our findings constitute, to our knowledge, the first molecular characterization of the trafficking mechanisms of a member of the mammalian aquaporin family in epithelial cells.

Two independent signals determine AQP4 basolateral targeting

We have shown that AQP4 is targeted to the basolateral membranes of our *in vitro* cellular model system (the MDCK cells) as was described *in vivo* in tracheal, kidney and gastric cells (Frigeri *et al*., 1995; Fujita *et al*., 1999). We found that the cytoplasmic sorting cassette of AQP4 contains two independent basolateral sorting signals. One signal consists of a di-leucine-based motif preceded by a cluster of acidic amino acids (ETEDLIL), while the other involves the tyrosine-based motif (YMEV). Previously characterized di-leucine-based basolateral sorting signals fall into to two categories. One type, described in the IgG Fc receptor and the human invariant chain, only requires a central di-hydrophobic doublet (LL and ML, respectively) (Hunziker and Fumey, 1994; Odorizzi and Trowbridge, 1997). The other type, seen in the endoprotease furin, requires, as in AQP4, an additional upstream acidic amino acid (Simmen *et al*., 1999). Although our results (Figure 4C) suggest a predominant role of the acidic cluster in the AQP4 sorting signal, both motifs are necessary to constitute the basolateral sorting signal. However, it should be noted that differential reading of leucine-based motifs has also been reported for endocytotic and lysosomal targeting motifs in other proteins (Sandoval *et al*., 2000).

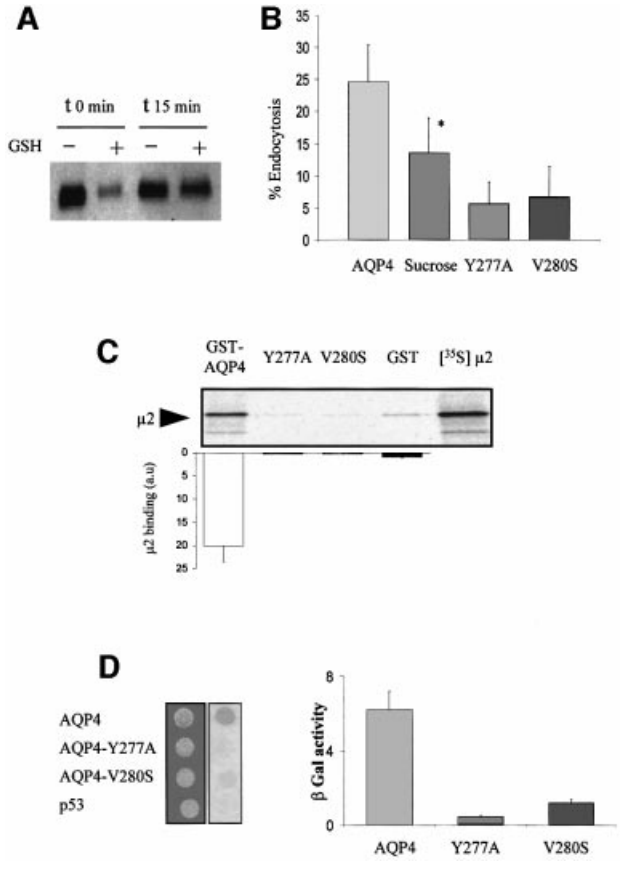

Fig. 5. AQP4 is endocytosed by clathrin-dependent mechanisms and interacts with the µ subunit of AP2 complex. (**A**) Western blot probed with anti-AQP4 antibody illustrating AQP4 endocytosis assay in MDCK cells assessed by biotinylation experiments. AQP4 was biotinylated at 4°C (t_0) and allowed to internalize for 15 min at 37°C (t_{15}). Endocytosed AQP4 was protected from glutathione reduction (+), isolated using streptavidin beads and quantified by western blotting using anti-AQP4. (**B**) Percentage of endocytosis measured for VSV-AQP4 in control and hyperosmotic conditions (AQP4 and Sucrose, respectively), Y277A and V280S mutants. Data represent the means ± SD of at least four experiments. * indicates significant difference against the control $p<0.05$ (paired Student's *t*-test). (**C**) Autoradiography of *in vitro* translated ^{35}S-labeled µ2 subunit retained by *in vitro* binding assay using 3 µg of control GST, GST–AQP4-Cter, GST–AQP4-Y277A (Y277A) and GST–AQP4-V280S (V280S) fusion proteins. One-fifth of the µ2 input used in the binding assay is shown in the right-hand lane ([^{35}S]µ2). Results are quantified in the histogram. Values on the ordinate are arbitrary units; the reference (GST) was assigned a value of 1. Assays were performed in triplicate. (**D**) Two-hybrid assay of AQP4–µ2 interaction. EGY48 yeast strain co-transformed with pACTII-µ2 and wild-type or mutants LEXA-AQP4 baits (AQP4, Y277A or V280S, respectively) were patched on selective medium, replica plated on Whatmann filters and tested for interaction using β-galactosidase activity (blue spots on right-hand image). LEXA-p53 fusion protein (p53) was used as a negative control. Right panel; the strength of interaction was quantified from β-gal activity measured in liquid culture. Values are expressed as means in arbitrary units/min/cell ± SD ($n = 4$) from three different yeast transformants.

We identified the tyrosine-based motif 275-GSYMEV-280 as the other basolateral sorting motif of AQP4. A subset of tyrosine-based basolateral sorting signals are those implicated in plasma membrane internalization, while others are not (Heilker *et al*., 1999; Yeaman *et al*., 1999). We found that the AQP4 basolateral sorting signal is co-linear with its endocytosis signal, as has been described for the asialoglycoprotein receptor (Geffen *et al*., 1993) and LampI (Honing and Hunziker, 1995). However, even though disruption of the tyrosine motif (Y277A and V280S) significantly altered AQP4 basolateral targeting, G275A substitution was necessary to completely re-route the protein to the apical membranes (Figure 3). This result may indicate that Gly275 is directly involved in the interaction of the signal with the sorting machinery (Ohno *et al*., 1996). Alternatively, structure prediction analysis anticipates that G275A mutation introduces important structural modifications in that critical region of the protein, suggesting a role of Gly275 in the broader structure of the interaction domain.

The polarized distribution of plasma membrane proteins in epithelial cells is maintained by sorting from intracellular compartments and selective retention in the membranes. To date, the intracellular machinery that reads di-leucine- and tyrosine-based basolateral sorting signals to accomplish protein sorting remains largely unknown. However, recent studies identified a novel form of the AP1 clathrin–adaptor complex (AP1-B), which contains an epithelial specific µ1B subunit. µ1B recognizes and specifically binds to the tyrosine-dependent signals involved in the basolateral targeting of the LDL receptor in MDCK cells (Folsch *et al*., 1999, 2001; Ohno *et al*., 1999). However, several unpublished observations from our group argue against a role of the AP1B complex in AQP4 basolateral targeting. Thus, the machinery that recognizes the peptidic sequences and/or the structural signatures of AQP4 basolateral sorting signals remains to be elucidated.

AQP4 is endocytosed and targeted to lysosomes

We found that AQP4 is efficiently internalized from the basolateral membrane of MDCK cells. Internalization has long been identified as an effective regulatory mechanism of water permeability in the principal cells of collecting ducts in the kidney. In these cells, the apical water channel AQP2 is endocytosed after vasopressin washout (Brown *et al*., 1988; Fushimi *et al*., 1997; Deen and Van Os, 1998). In a recent study, Carmosino *et al*. (2001) suggest that endocytosis is involved in AQP4 orthogonal array rearrangements of gastric cells in response to histamine treatment. However, the molecular mechanisms involved in aquaporin internalization are not completely clarified yet. Here, we identified the tyrosine motif 277-YMEV-280 as the critical endocytosis signal of AQP4 and have shown that this motif interacts directly with an essential actor of the plasma membrane protein internalization machinery: the µ subunit of the AP2 clathrin–adaptor complex. Whereas our data represent the first molecular characterization of the mechanisms involved in aquaporin endocytosis, such direct interaction of plasma membrane transporters with clathrin-dependent endocytosis machinery components is not unprecedented and has been documented for the epithelial sodium channel and cystic fibrosis transmembrane regulator (Shimkets *et al*., 1997; Weixel and Bradbury, 2000).

Once endocytosed, plasma membrane proteins may be either recycled back to the cell surface or further transported along the endocytic pathway down to lysosomes. Here, we found that AQP4 was efficiently targeted to the late endosomal/lysosomal compartment,

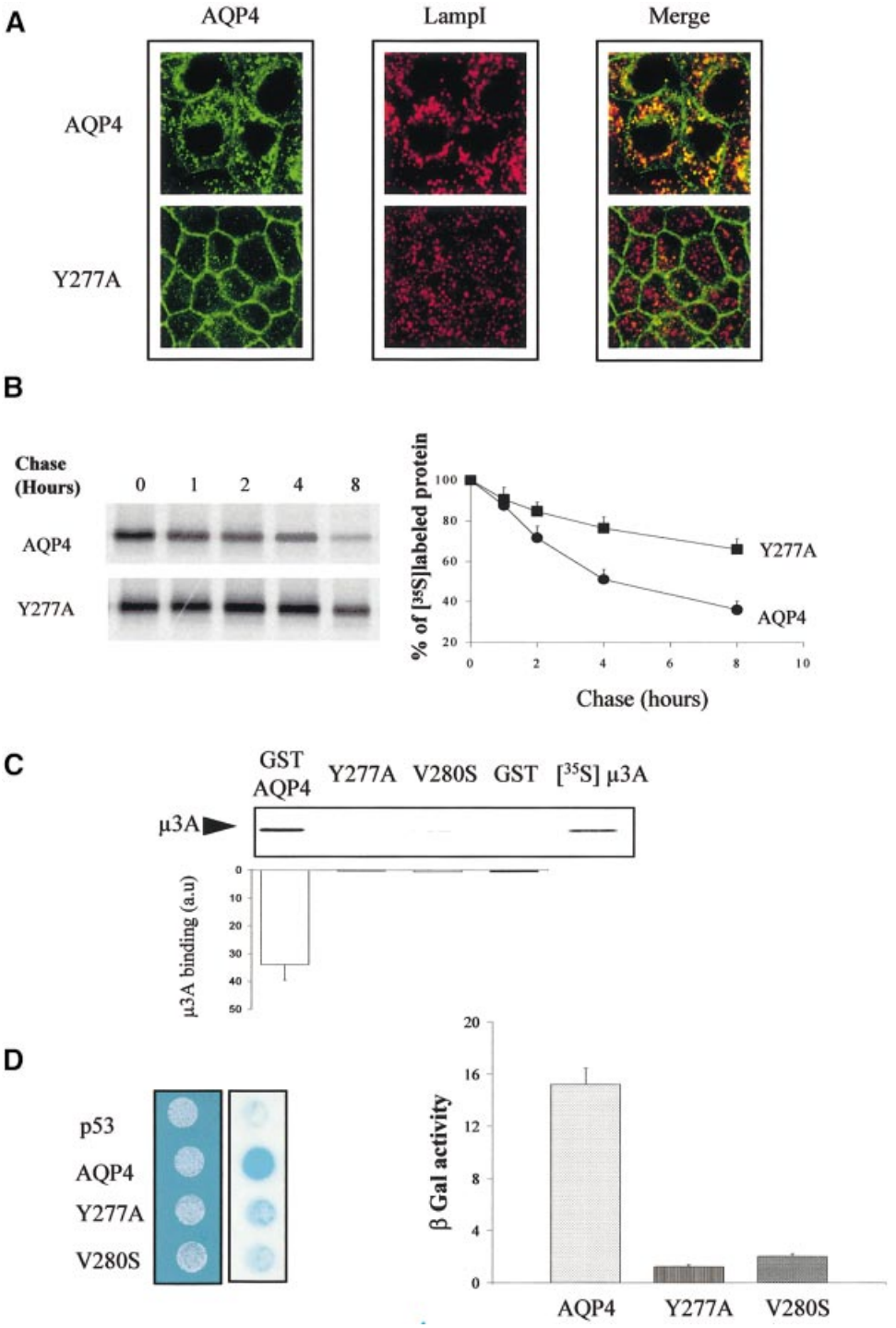

Fig. 6. AQP4 is targeted to lysosomes and interacts with µ3A. (**A**) Confocal microscopy images of wild-type VSV-AQP4 (AQP4, top images) and VSV-AQP4-Y277A (Y277A, bottom images) labeled with anti-VSV antibody (green) and anti-LampI antibody (red). Co-localization is shown as yellow staining in the merged right-hand images. (**B**) Left panel: autoradiography of wild-type VSV-AQP4 and AQP4-Y277A mutant proteins pulse-labeled with [^{35}S]methionine, chased for 0–8 h and immunoprecipitated using anti-VSV antibody. Right panel: radioactivity of the bands was quantified and the results are expressed in percent of the radioactivity measured at t_0. Data are the means ± SD of at least three experiments. (**C**) Autoradiography of *in vitro* translated ^{35}S-labeled µ3A subunit retained by *in vitro* binding assay using 3 µg of control GST, GST–AQP4-Cter, GST–AQP4-Y277A and V280S mutant fusion proteins. The quantification shown on the histogram was performed according to Figure 5C. (**D**) Two-hybrid assay of AQP4–µ3A interaction. Left panel; EGY48 yeast strain co-transformed with pACTII-µ3A and wild-type or mutant LEXA-AQP4 baits (AQP4, Y277A or V280S, respectively) were patched on selective medium, replica plated on Whatmann filters and tested for interaction using β-galactosidase activity (blue spots on right-hand image). LEXA-p53 fusion protein (p53) was used as a negative control. Right panel: the strength of interaction was quantified from β-gal activity measured in liquid culture. Values are expressed as means in arbitrary units/min/cell ± SD (n = 5) from three different yeast transformants.

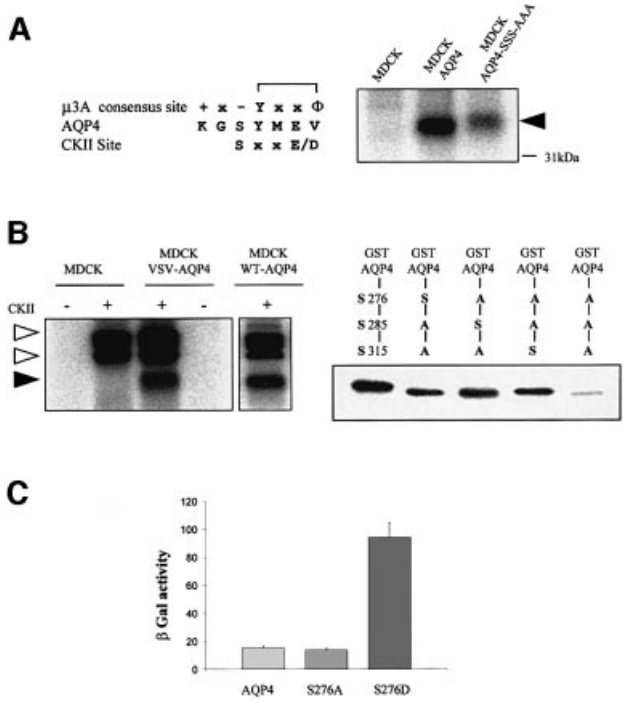

Fig. 7. CKII phosphorylates AQP4 and modulates AQP4–μ3A interaction. (**A**) Left panel: sequence alignment of tyrosine-based motif favored by μ3A, amino acid sequence surrounding the AQP4 tyrosine-based motif and CKII consensus site. Right panel: autoradiography of wild-type AQP4 and AQP4-SSS-AAA mutant immunoprecipitated using the anti-VSV antibody from cells labeled with [^{32}P]ortho-phosphate and exhibiting similar AQP4-expression level. A ^{32}P-labeled AQP4 (arrowhead) was immunoprecipitated from VSV-AQP4 transfected cells (MDCK-AQP4) but not from control MDCK cells. (**B**) *In vitro* phosphorylation of AQP4 and GST–AQP4-Cter by CKII using γ-[^{32}P]ATP. Left panel: AQP4 protein immunoprecipitated from VSV-AQP4-MDCK cells and control MDCK cells (using anti-VSV antibody) and WT-AQP4-MDCK cells (using anti-AQP4 antibody) were incubated with (+) or without (–) CKII in the presence of [^{32}P]γ-ATP. Open and filled arrowheads indicate autophosphorylated CKII subunits and ^{32}P-labeled AQP4, respectively. Right panel: GST–AQP4-Cter fusion proteins containing, either wild-type AQP4 (left lane) or mutant AQP4 sequences in which only one of the three potential CKII sites (Ser275, Ser285 and Ser315) was conserved, were phosphorylated by CKII in the presence of [^{32}P]γ-ATP. GST–AQP4-Cter fusion protein in which the three serines were replaced by alanines exhibited background level of phosphorylation (last lane). (**C**) Strength of interaction measured in the yeast two-hybrid assay between μ3A and wild-type AQP4 (AQP4) and the mutant baits S276A and S276D. Values are expressed means ± SD (n = at least five in each group) in arbitrary units/min/cell.

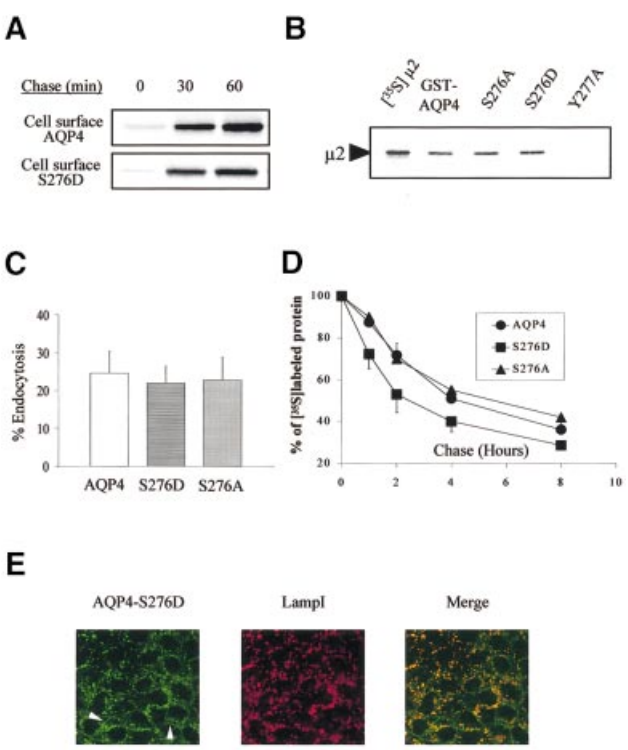

Fig. 8. CKII phosphorylation increases AQP4 lysosomal targeting and degradation but not endocytosis. (**A**) Cell surface delivery of VSV-AQP4 and S276D mutant revealed in pulse–chase experiments coupled to cell surface biotinylation. Both newly synthesized proteins were detected on the cell surface after a 30 min chase period. (**B**) Autoradiography of *in vitro* translated ^{35}S-labeled μ2 subunit retained on 3 μg of wild-type GST–AQP4-Cter and the mutant constructs S276A and S276D. GST–AQP4-Y277A was used as a negative control (last lane). One fifth of the μ2 translation reaction used in the assay is shown in the left-hand lane ([^{35}S]μ2). (**C**) Percentage of endocytosis of AQP4 measured in wild-type AQP4, AQP4-S276D and AQP4-S276A-MDCK cells using the biotinylation protocol. Values are expressed means ± SD (n = at least three in each group). (**D**) Degradation rate measured in pulse–chase experiments for wild-type AQP4, S276D and S276A mutants. Results are expressed as a percentage of the radioactivity measured at t_0 (see Figure 5). (**E**) Confocal images of AQP4-S276D-MDCK cells processed using anti-VSV (green) and anti-LampI antibody (red). Co-localization is shown as yellow staining in merged right-hand image. Arrowheads point to visible AQP4 basolateral expression.

where it co-localized with LampI (Nabi *et al*., 1991). In addition, we demonstrated that the AQP4 C-terminus interacted directly with the μ3A subunit of the AP3 adaptor complex involved in protein targeting to the lysosomes (Le Borgne *et al*., 1998; Odorizzi *et al*., 1998). The observation that AQP4 lysosomal localization, degradation rate and interaction with μ3A subunit were dramatically affected by the Y277A substitution strongly supports the idea of an effective role of the tyrosine-based motif in AQP4 intracellular traffic. In addition, we showed that AQP4 endocytosis was reduced by 80% when the Tyr277 was replaced by an alanine (Y277A). This identified the tyrosine motif as the critical endocytosis signal of AQP4 and indicated that the di-leucine-like motif plays little or no role in this process. This notion was further sustained by: (i) pull-down experiments showing a large decrease (>90%) of μ2 binding to GST–AQP4-Y277A fusion protein despite the presence of the di-leucine motif in this fusion protein; and (ii) our inability to detect μ2–AQP4 interaction in a yeast two-hybrid assay using different baits specifically containing the di-leucine motif (our unpublished data). Also, we could not detect any interaction with the μ1A subunit of AP1 complexes (not shown).

Altogether, these results argue in favor of serial interactions of the tyrosine motif with AP2 and then AP3 complexes signaling AQP4 endocytosis and lysosomal targeting, respectively. Such a mechanism suggests that regulatory cues must somehow modulate these trafficking steps to control plasma membrane water permeability efficiently.

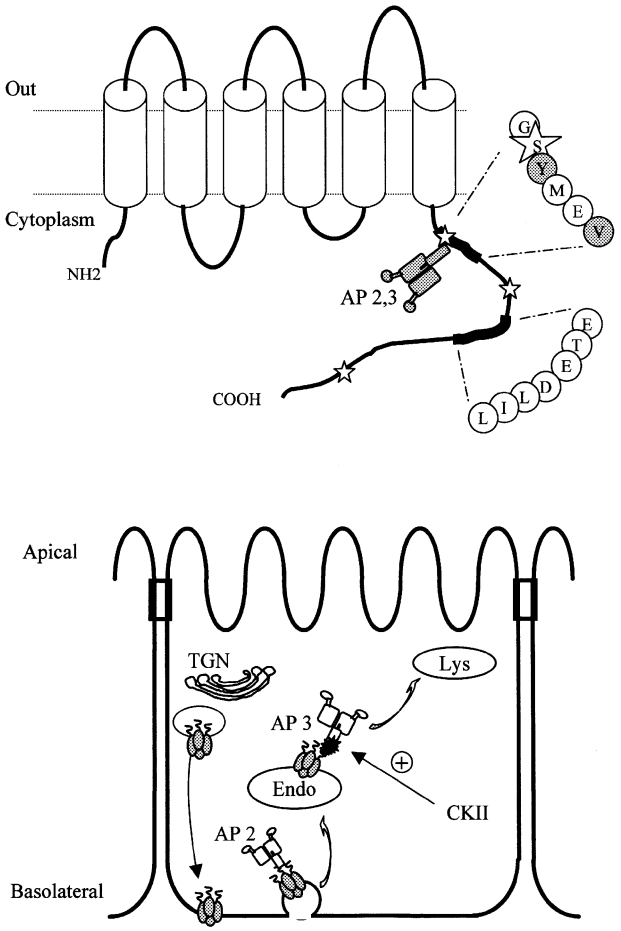

Fig. 9. Schematic illustration of AQP4 sorting motifs and trafficking in epithelial cells. Upper panel: hydropathy analysis of AQP4 sequence predicted six transmembrane domains connected by five loops. The two C-terminal basolateral targeting motifs (GSYMEV and ETEDLIL) are shown. Stars indicate the three serines phosphorylated by CKII. The adaptor complexes (AP2 and AP3) interacting with the tyrosine-based motif are shown. The residues critical for AQP4–μ subunits interactions (Y277 and V280) are shaded. Lower panel: model of AQP4 trafficking in epithelial cells. *Trans*-Golgi network (TGN), endosomal (Endo) and lysosomal (Lys) compartments are shown.

CKII regulates AQP4 trafficking along the endocytic pathway

Consistent with this hypothesis, we found that AQP4 is phosphorylated in MDCK cells. In addition, we established that AQP4 is phosphorylated efficiently by recombinant human CKII *in vitro*, in particular on Ser276 located just upstream of the tyrosine motif. Furthermore, we showed that S276D substitution, used to mimic serine phosphorylation, did not affect delivery of newly synthesized protein, but increased AQP4–μ3A interaction, lysosomal localization and AQP4 degradation. This suggests that the traffic from an endosomal compartment to lysosomes is indeed regulated by CKII. However, we can not exclude a possible direct lysosomal targeting from the TGN through the AP3 adaptor complex. Involvement of CKII in different aspects of membrane protein trafficking has already been documented. For instance, CKII phosphorylation of varicella–zoster virus glycoprotein (Alconada *et al*., 1996), the furin (Jones *et al*., 1995) or the cation-dependent mannose-6-phosphate receptor (Mauxion *et al*., 1996) modulates their interactions with components of the clathrin-mediated sorting machinery like members of the phosphofurin acidic cluster sorting protein family (PACS) protein family (Wan *et al*., 1998). Also, CKII has been reported to regulate the degradation of a number of proteins, including lens connexins (Yin *et al*., 2000).

Putative physiological role of CKII-regulated AQP4 trafficking

Several observations suggest that the modulation of AQP4 trafficking by CKII might play a role in brain recovery after ischemic insults and edema formation. In fact, according to Manley *et al*. (2000), AQP4 gene deletion significantly improves neurological outcome after water intoxication and ischemic stroke. In addition, ischemic stress induces the disappearance of OAPs, now known to contain AQP4, from brain astrocyte membrane (Landis and Reese, 1981; Verbavatz *et al*., 1997; Rash *et al*., 1998), and increased CKII activity has been reported in brain ischemia. A close correlation was also established between improved cellular survival and high CKII activity in brain regions resistant to ischemia (Hu and Wieloch, 1993; Johnson, 1998). Altogether, these data suggest that CKII phosphorylation may participate in the down-regulation of AQP4 and play a role in the cellular responses to brain ischemia. Further studies will be required to ascertain this point.

In conclusion, we have identified in the cytoplasmic C-terminus of AQP4 a unique sorting cassette (Figure 9). This domain contains several distinct signals that coordinate polarized basolateral targeting in epithelial cells, and regulate cell surface expression by endocytosis and lysosomal degradation. Basolateral targeting is mediated by two independent signals. One is encoded by a dileucine-like motif preceded by a cluster of acidic residues (ETEDLIL). The other basolateral sorting signal overlaps with a tyrosine-based endocytic motif (GSYMEV). This latter motif serially interacts with the μ2 and μ3 subunits of the clathrin–adaptor complexes AP2 and AP3, signalling endocytosis and lysosomal targeting, respectively. CKII phosphorylation of AQP4 increases interaction with the AP3 clathrin–adaptor complex, enhancing AQP4 targeting to lysosomes. Our data have highlighted molecular and cellular mechanisms of regulation of an essential actor of brain edema formation that may have therapeutic ramifications.

Materials and methods

cDNA constructs and mutagenesis

The cDNA encoding the rat AQP4 protein was amplified by PCR from a rat kidney cDNA library and cloned in the expression vector pCB6. A VSV epitope-tagged AQP4 was generated by introducing the nucleotide sequence encoding the 11 amino acids of the VSV tag just after the initiation codon of AQP4 cDNA. The VSV epitope was modified to disrupt a potential sorting signal, as already described (Le Maout *et al*., 1997). Mutations listed in Table I were made by PCR-based mutagenesis or using the QuikChange™ site-directed mutagenesis kit (Stratagene) according to the manufacturer's specifications. All the constructs were verified by DNA sequencing.

Transfection and stable cell line generation

MDCK cells were grown in Dulbecco's modified Eagle's medium (DMEM) supplemented with 10% fetal bovine serum (FBS). They were

transfected with 2 μg of recombinant PCB6 plasmid using Superfect (Qiagen). Stable transfected MDCK cells clones were isolated in a selection medium containing 500 μg/ml G418 (BRL). Control MDCK cell clones were obtained by the same transfection protocol using the pCB6 plasmid alone.

Immunofluorescence and confocal microscopy

For immunofluorescence experiments, cells were grown on permeable supports until they formed a confluent monolayer. They were fixed with 3% paraformaldehyde and permeabilized with 0.1% Triton X-100 in phosphate-buffered saline (PBS). They were then incubated with the P5D4 antibody (1:1000; Sigma) directed against the VSV epitope. In co-localization experiments with LampI, the cells were sequentially processed with the AC17 anti-LampI antibody (1/1000) (Nabi *et al*., 1991), revealed by fluorescein-conjugated anti-mouse antibody, and then with biotinylated P5D4 antibody (1/1000), which was revealed using Texas Red-conjugated streptavidin (1/200). Confocal microscope analysis was performed on a LSM Zeiss confocal microscope.

Western blots, metabolic labeling and immunoprecipitation

Cells were lysed with 150 mM NaCl, 20 mM Tris, 5 mM EDTA pH 7.5, supplemented with 1% Triton X-100, 0.1% bovine serum albumin (BSA) and a protease inhibitor cocktail (antipain, leupeptin and pepstatin 10 μg/ml each, and 1 mM phenylmethylsulfonyl fluoride). The protein concentration was determined using the BCA Protein Assay Reagent kit (Pierce). The proteins were denatured by heating at 50°C for 15 min in Laemmli sample buffer, separated by SDS–PAGE on 12% gels and transferred to nitrocellulose membranes (Schleicher and Schuell). The blots were probed with the affinity-purified anti-AQP4 (1/2000) raised against the C-terminal amino acids of the protein (aa: KKGKDSSGEVLSSV, Valenti *et al*., 1996) and secondary horseradish peroxidase-coupled antibody. The proteins were then visualized using the enhanced chemiluminescence kit (NEN).

For metabolic labeling experiments, the cells were incubated at 37°C for 30 min in cysteine- and methionine-free DMEM (Life Technologies), and then pulse labeled for 10 min at 37°C with 500 μCi/ml [^{35}S]methionine and [^{35}S]cysteine (Express Protein Labeling Mix, NEN). After washings in DMEM, they were chased for 1–10 h in DMEM supplemented with 10% FBS and a 10-fold excess of cold methionine and cysteine. After three washes in PBS at 4°C, cells were lysed as described above. AQP4 proteins were immunoprecipitated using P5D4 antibody (1/1000) and protein A–Sepharose beads, separated by SDS–PAGE and the radioactivity quantified on a phosphoimager (Amersham Pharmacia).

Cell surface biotinylation in endocytosis assays and pulse–chase experiments

In endocytosis assays, confluent monolayers were incubated twice with the cleavable EZ-Link Sulfo-NHS-SS-Biotin (0.5 mg/ml) (Pierce) in 125 mM NaCl, 10 mM tri-ethanolamine, 2 mM $CaCl_2$ pH 9.0 for 20 min at 4°C. After washing, the cells were incubated at 37°C for 15 min in DMEM supplemented with 10% FBS and 0.1% BSA. Cells were rapidly rinsed with cold PBS and incubated at 4°C for 20 min with the impermeant reducing agent glutathione (50 mM) in 75 mM NaCl, 75 mM NaOH to cleave the biotin bound to non-endocytosed proteins. This procedure was repeated twice and the cells were then incubated for 20 min in PBS supplemented with 1% BSA and 50 mM iodoacetamide to quench free SH groups. The cells were lysed as described above and biotinylated proteins recovered using streptavidin–agarose beads (Pharmacia). After washing, the bound proteins were eluted with Laemmli sample buffer, separated by SDS–PAGE on 12% gels, transferred to nitrocellulose and the blots probed with anti-AQP4 antibody as described above. The blots were quantified using a Fluorchem 8000 system (Alpha Innotech Corp). In a typical experiment, eight cultures were used. After biotinylation, four were kept at 4°C and four incubated at 37°C for 15 min. Two cultures of each batch were reduced with glutathione ($t0_{red}$, $t15_{red}$). Non-reduced t15 (t15) and reduced t0 ($t0_{red}$) cultures were used to estimate spontaneous de-biotinylation of the protein during incubation at 37°C (usually <2%) and background, respectively. Results are expressed as the percentage of endocytosis, calculated as $\%Endo = (t15_{red} - t0_{red}) \times 100/t0$. The values presented are the mean of at least four experiments carried out on at least two different clonal cells lines. Hypertonic sucrose (0.45 M) treatment was performed according to Hansen *et al*. (1993).

In pulse–chase experiments coupled to cell surface biotinylation, cells were pulse labeled as described above and chased for 30 and 60 min. Apical or basolateral membranes were treated with non-cleavable EZ-Link Sulfo-NHS-Biotin (0.5 mg/ml; Pierce), biotinylated proteins harvested with streptavidin–agarose, and newly synthesized AQP4 immunoprecipitated using anti-VSV antibody. Proteins were separated by PAGE and quantified on a phosphoimager as described above.

To quantify steady-state apical versus basolateral expression of AQP4 mutants, cells were treated with non-cleavable biotin from the apical or the basolateral side. Biotinylated proteins were isolated with streptavidin–agarose, processed for western blotting using anti-AQP4 and quantified using the Fluorchem 8000 system as described above.

In vitro binding and yeast two-hybrid interaction assays

The cDNA encoding the entire AQP4 C-terminus (V251–V323) was cloned in-frame into the pGEX-3 vector (Pharmacia) to produce GST–AQP4-Cter fusion proteins in BL21 *Escherichia coli*. Mutant GST–AQP4-Cter proteins were constructed using the QuikChange™ Site-Directed Mutagenesis Kit (Stratagene). The fusion proteins were purified on glutathione–Sepharose beads (Pharmacia). The μ subunit of AP2 and AP3 complexes cloned into pSG vector (Le Gall *et al*., 1998) was produced using the TnT-coupled reticulocyte lysate system (Promega) in the presence of [^{35}S]methionine. For *in vitro* binding experiments, 3 μg of bound GST–AQP4 fusion protein were incubated for q h at 4°C with ^{35}S-labeled μ2 or μ3A proteins, and then washed three times with 150 mM NaCl, 20 mM Tris, 5 mM EDTA pH 8.0 supplemented with 2% BSA, and twice in the same buffer without BSA. Bound μ2 and μ3A proteins were eluted with 30 μl of Laemmli sample buffer, separated by SDS–PAGE on 8% gels and analyzed on a phosphoimager (Amersham Pharmacia).

For the yeast two-hybrid assay, the cDNA encoding the entire AQP4 C-terminus (V251–V323) or the fragment V251–E281 was subcloned in-frame with the LEXA DNA binding domain into the pLEXA plasmid (Clontech) to generate pLEXA-AQP4 vector. Y277A, S276D, S276A and V280S substitutions were introduced into pLEXA-AQP4 using the QuikChange™ Mutagenesis kit (Stratagene). The μ3A subunit was fused to the Gal4 activation domain in the pACTII vector (Le Gall *et al*., 1998).

The EGY48 yeast reporter strain containing the *LacZ* LexA inducible gene was co-transformed with the indicated pLEXA-AQP4 and Gal4-μ3A hybrid expression vectors and then plated on selective medium lacking histidine and leucine. Double transformants were then patched on the same medium and analyzed for qualitative β-galactosidase activity on Whatman filters. The liquid culture assay for quantitative β-galactosidase activity was performed using 2-nitrophenyl-β-D-galactopyranoside as a substrate (Erdtmann *et al*., 2000).

Phosphorylation assays

The cells were phosphate depleted by a 30 min incubation at 37°C in phosphate-free DMEM. They were labeled with 200 μCi of [^{32}P]orthophosphate at 37°C for 2 h and then lysed using a lysis buffer containing in addition 1 mM sodium pyrophosphate, 1 mM sodium fluoride and 300 nM okadaic acid. AQP4 protein was immunoprecipitated as described above using P5D4 antibody, separated by PAGE on 10% gels and analyzed on a phosphoimager (Amersham Pharmacia). For *in vitro* phosphorylation experiments, immunoprecipitated AQP4 and GST–AQP4 fusion proteins (2 μg) were incubated for 15 min at 30°C with recombinant human CKII (Calbiochem) in the presence of 10 μCi of [γ-^{32}P]ATP and 0.4 μM polylysine.

Acknowledgements

We thank A.Frigeri and G.Valenti for the kind gift of anti-AQP4 antibody, and P.A.Welling for his critical review of the manuscript. We also thank C.Klein (INSERM-IFR58 Institut des Cordeliers, Paris) for his excellent assistance in confocal microscope experiments. This work was supported by the European TMR project FMRX-CT970128.

References

Alconada,A., Bauer,U. and Hoflack,B. (1996) A tyrosine-based motif and a casein kinase II phosphorylation site regulate the intracellular trafficking of the varicella-zoster virus glycoprotein I, a protein localized in the *trans*-Golgi network. *EMBO J.*, **15**, 6096–6110.

Brown,D. and Breton,S. (2000) Sorting proteins to their target membranes. *Kidney Int.*, **57**, 816–824.

Brown,D., Weyer,P. and Orci,L. (1988) Vasopressin stimulates endocytosis in kidney collecting duct principal cells. *Eur. J. Cell Biol.*, **46**, 336–341.

Carmosino,M., Procino,G., Nicchia,G.P., Manucci,R., Verbavatz,J.M.,

Gobin,R., Svelto,M. and Valenti,G. (2001) Histamine treatment induces rearrangements of orthogonal arrays of particles (OAPs) in human AQP4-expressing gastric cells. *J. Cell Biol.*, **154**, 1235–1243.

Deen,P.M. and van Os,C.H. (1998) Epithelial aquaporins. *Curr. Opin. Cell Biol.*, **10**, 435–442.

Engel,A., Fujiyoshi,Y. and Agre,P. (2000) The importance of aquaporin water channel protein structures. *EMBO J.*, **19**, 800–806.

Erdtmann,L., Janvier,K., Raposo,G., Craig,H.M., Benaroch,P., Berlioz-Torrent,C., Guatelli,J.C., Benarous,R. and Benichou,S. (2000) Two independent regions of HIV-1 Nef are required for connection with the endocytic pathway through binding to the mu 1 chain of AP1 complex. *Traffic*, **1**, 871–883.

Folsch,H., Ohno,H., Bonifacino,J.S. and Mellman,I. (1999) A novel clathrin adaptor complex mediates basolateral targeting in polarized epithelial cells. *Cell*, **99**, 189–198.

Folsch,H., Pypaert,M., Schu,P. and Mellman,I. (2001) Distribution and function of AP-1 clathrin adaptor complexes in polarized epithelial cells. *J. Cell Biol.*, **152**, 595–606.

Frigeri,A., Gropper,M.A., Turck,C.W. and Verkman,A.S. (1995) Immunolocalization of the mercurial-insensitive water channel and glycerol intrinsic protein in epithelial cell plasma membranes. *Proc. Natl Acad. Sci. USA*, **92**, 4328–4331.

Fujita,A., Horio,Y., Nielsen,S., Nagelhus,E.A., Hata,F., Ottersen,O.P. and Kurachi,Y. (1999) High-resolution immunogold cytochemistry indicates that AQP4 is concentrated along the basal membrane of parietal cells in rat stomach. *FEBS Lett.*, **459**, 305–309.

Fushimi,K., Sasaki,S. and Marumo,F. (1997) Phosphorylation of serine 256 is required for cAMP-dependent regulatory exocytosis of the aquaporin-2 water channel. *J. Biol. Chem.*, **272**, 14800–14804.

Geffen,I., Fuhrer,C., Leitinger,B., Weiss,M., Huggel,K., Griffiths,G. and Spiess,M. (1993) Related signals for endocytosis and basolateral sorting of the asialoglycoprotein receptor. *J. Biol. Chem.*, **268**, 20772–20777.

Hansen,S.H., Sandvig,K. and van Deurs,B. (1993) Clathrin and HA2 adaptors: effects of potassium depletion, hypertonic medium and cytosol acidification. *J. Cell Biol.*, **121**, 61–72.

Heilker,R., Spiess,M. and Crottet,P. (1999) Recognition of sorting signals by clathrin adaptors. *BioEssays*, **21**, 558–567.

Honing,S. and Hunziker,W. (1995) Cytoplasmic determinants involved in direct lysosomal sorting, endocytosis and basolateral targeting of rat lgp120 (lamp-I) in MDCK cells. *J. Cell Biol.*, **128**, 321–332.

Hu,B.R. and Wieloch,T. (1993) Casein kinase II activity in the postischemic rat brain increases in brain regions resistant to ischemia and decreases in vulnerable areas. *J. Neurochem.*, **60**, 1722–1728.

Hunziker,W. and Fumey,C. (1994) A di-leucine motif mediates endocytosis and basolateral sorting of macrophage IgG Fc receptors in MDCK cells. *EMBO J.*, **13**, 2963–2967.

Johnson,T.D. (1998) Polyamines and cerebral ischemia. *Prog. Drug Res.*, **50**, 193–258.

Jones,B.G., Thomas,L., Molloy,S.S., Thulin,C.D., Fry,M.D., Walsh,K.A. and Thomas,G. (1995) Intracellular trafficking of furin is modulated by the phosphorylation state of a casein kinase II site in its cytoplasmic tail. *EMBO J.*, **14**, 5869–5883.

Jung,J.S., Bhat,R.V., Preston,G.M., Guggino,W.B., Baraban,J.M. and Agre,P. (1994) Molecular characterization of an aquaporin cDNA from brain: candidate osmoreceptor and regulator of water balance. *Proc. Natl Acad. Sci. USA*, **91**, 13052–13056.

Ke,C., Poon,W.S., Ng,H.K., Pang,J.C. and Chan,Y. (2001) Heterogeneous responses of aquaporin-4 in oedema formation in a replicated severe traumatic brain injury model in rats. *Neurosci. Lett.*, **301**, 21–24.

Landis,D.M. and Reese,T.S. (1981) Astrocyte membrane structure: changes after circulatory arrest. *J. Cell Biol.*, **88**, 660–663.

Le Borgne,R., Alconada,A., Bauer,U. and Hoflack,B. (1998) The mammalian AP-3 adaptor-like complex mediates the intracellular transport of lysosomal membrane glycoproteins. *J. Biol. Chem.*, **273**, 29451–29461.

Le Gall,S., Erdtmann,L., Benichou,S., Berlioz-Torrent,C., Liu,L., Benarous,R., Heard,J.M. and Schwartz,O. (1998) Nef interacts with the mu subunit of clathrin adaptor complexes and reveals a cryptic sorting signal in MHC I molecules. *Immunity*, **8**, 483–495.

Le Maout,S., Brejon,M., Olsen,O., Merot,J. and Welling,P.A. (1997) Basolateral membrane targeting of a renal-epithelial inwardly rectifying potassium channel from the cortical collecting duct, CCD-IRK3, in MDCK cells. *Proc. Natl Acad. Sci. USA*, **94**, 13329–13334.

Manley,G.T., Fujimura,M., Ma,T., Noshita,N., Filiz,F., Bollen,A.W., Chan,P. and Verkman,A.S. (2000) Aquaporin-4 deletion in mice reduces brain edema after acute water intoxication and ischemic stroke. *Nature Med.*, **6**, 159–163.

Mauxion,F., Le Borgne,R., Munier-Lehmann,H. and Hoflack,B. (1996) A casein kinase II phosphorylation site in the cytoplasmic domain of the cation-dependent mannose 6-phosphate receptor determines the high affinity interaction of the AP-1 Golgi assembly proteins with membranes. *J. Biol. Chem.*, **271**, 2171–2178.

Nabi,I.R., Le Bivic,A., Fambrough,D. and Rodriguez-Boulan,E. (1991) An endogenous MDCK lysosomal membrane glycoprotein is targeted basolaterally before delivery to lysosomes. *J. Cell Biol.*, **115**, 1573–1584.

Nagelhus,E.A., Veruki,M.L., Torp,R., Haug,F.M., Laake,J.H., Nielsen,S., Agre,P. and Ottersen,O.P. (1998) Aquaporin-4 water channel protein in the rat retina and optic nerve: polarized expression in Muller cells and fibrous astrocytes. *J. Neurosci.*, **18**, 2506–2519.

Nagelhus,E.A., Horio,Y., Inanobe,A., Fujita,A., Haug,F.M., Nielsen,S., Kurachi,Y. and Ottersen,O.P. (1999) Immunogold evidence suggests that coupling of K^+ siphoning and water transport in rat retinal Muller cells is mediated by a coenrichment of Kir4.1 and AQP4 in specific membrane domains. *Glia*, **26**, 47–54.

Neely,J.D., Christensen,B.M., Nielsen,S. and Agre,P. (1999) Heterotetrameric composition of aquaporin-4 water channels. *Biochemistry*, **38**, 11156–11163.

Odorizzi,G. and Trowbridge,I.S. (1997) Structural requirements for major histocompatibility complex class II invariant chain trafficking in polarized Madin-Darby canine kidney cells. *J. Biol. Chem.*, **272**, 11757–11762.

Odorizzi,G., Cowles,C.R. and Emr,S.D. (1998) The AP-3 complex: a coat of many colours. *Trends Cell Biol.*, **8**, 282–288.

Ohno,H., Fournier,M.C., Poy,G. and Bonifacino,J.S. (1996) Structural determinants of interaction of tyrosine-based sorting signals with the adaptor medium chains. *J. Biol. Chem.*, **271**, 29009–29015.

Ohno,H., Aguilar,R.C., Yeh,D., Taura,D., Saito,T. and Bonifacino,J.S. (1998) The medium subunits of adaptor complexes recognize distinct but overlapping sets of tyrosine-based sorting signals. *J. Biol. Chem.*, **273**, 25915–25921.

Ohno,H. *et al*. (1999) Mu1B, a novel adaptor medium chain expressed in polarized epithelial cells. *FEBS Lett.*, **449**, 215–220.

Rapoport,I., Chen,Y.C., Cupers,P., Shoelson,S.E. and Kirchhausen,T. (1998) Dileucine-based sorting signals bind to the beta chain of AP-1 at a site distinct and regulated differently from the tyrosine-based motif-binding site. *EMBO J.*, **17**, 2148–2155.

Rash,J.E., Yasumura,T., Hudson,C.S., Agre,P. and Nielsen,S. (1998) Direct immunogold labeling of aquaporin-4 in square arrays of astrocyte and ependymocyte plasma membranes in rat brain and spinal cord. *Proc. Natl Acad. Sci. USA*, **95**, 11981–11986.

Sandoval,I.V., Martinez-Arca,S., Valdueza,J., Palacios,S. and Holman, G.D. (2000) Distinct reading of different structural determinants modulates the dileucine-mediated transport steps of the lysosomal membrane protein LIMPII and the insulin-sensitive glucose transporter GLUT4. *J. Biol. Chem.*, **275**, 39874–39885.

Sheng,M. and Kim,E. (2000) The Shank family of scaffold proteins. *J. Cell Sci.*, **113**, 1851–1856.

Shimkets,R.A., Lifton,R.P. and Canessa,C.M. (1997) The activity of the epithelial sodium channel is regulated by clathrin-mediated endocytosis. *J. Biol. Chem.*, **272**, 25537–25541.

Simmen,T., Nobile,M., Bonifacino,J.S. and Hunziker,W. (1999) Basolateral sorting of furin in MDCK cells requires a phenylalanine–isoleucine motif together with an acidic amino acid cluster. *Mol. Cell. Biol.*, **19**, 3136–3144.

Vajda,Z., Promeneur,D., Doczi,T., Sulyok,E., Frokiaer,J., Ottersen,O.P. and Nielsen,S. (2000) Increased aquaporin-4 immunoreactivity in rat brain in response to systemic hyponatremia. *Biochem. Biophys. Res. Commun.*, **270**, 495–503.

Valenti,G., Frigeri,A., Ronco,P.M., D'Ettorre,C. and Svelto,M. (1996) Expression and functional analysis of water channels in a stably AQP2-transfected human collecting duct cell line. *J. Biol. Chem.*, **271**, 24365–24370.

van Hoek,A.N., Ma,T., Yang,B., Verkman,A.S. and Brown,D. (2000) Aquaporin-4 is expressed in basolateral membranes of proximal tubule S3 segments in mouse kidney. *Am. J. Physiol. Renal Physiol.*, **278**, F310–F316.

Venero,J.L., Vizuete,M.L., Machado,A. and Cano,J. (2001) Aquaporins in the central nervous system. *Prog. Neurobiol.*, **63**, 321–336.

Verbavatz,J.M., Ma,T., Gobin,R. and Verkman,A.S. (1997) Absence of orthogonal arrays in kidney, brain and muscle from transgenic knockout mice lacking water channel aquaporin-4. *J. Cell Sci.*, **110**, 2855–2860.

Wan,L., Molloy,S.S., Thomas,L., Liu,G., Xiang,Y., Rybak,S.L. and Thomas,G. (1998) PACS-1 defines a novel gene family of cytosolic sorting proteins required for trans-Golgi network localization. *Cell*, **94**, 205–216.

Weixel,K.M. and Bradbury,N.A. (2000) The carboxyl terminus of the cystic fibrosis transmembrane conductance regulator binds to AP-2 clathrin adaptors. *J. Biol. Chem.*, **275**, 3655–3660.

Yeaman,C., Grindstaff,K.K. and Nelson,W.J. (1999) New perspectives on mechanisms involved in generating epithelial cell polarity. *Physiol. Rev.*, **79**, 73–98.

Yin,X., Jedrzejewski,P.T. and Jiang,J.X. (2000) Casein kinase II phosphorylates lens connexin 45.6 and is involved in its degradation. *J. Biol. Chem.*, **275**, 6850–6856.

Received May 9, 2001; revised October 1, 2001; accepted October 24, 2001